



ELSEVIER

Catalysis Today 43 (1998) 249–259



## TPD and XRD studies of molybdenum nitride and its activity for hydrodenitrogenation of carbazole

Masatoshi Nagai\*, Yosuke Goto<sup>1</sup>, Osamu Uchino<sup>2</sup>, Shinzo Omi

*Department of Advanced Materials, Graduate School of Bio-Applications and Systems Engineering,  
Tokyo University of Agriculture and Technology, Koganei, Tokyo 184, Japan*

### Abstract

The nitrated  $\text{MoO}_3$  catalysts formed using two kinds of treatment with either  $\text{NH}_3$  or He after nitriding were studied by temperature-programmed desorption and X-ray diffraction analyses. The catalysts were cooled to room temperature in either flowing  $\text{NH}_3$  or He (NH or HE catalyst) after nitriding at 773, 973 and 1173 K with  $\text{NH}_3$ . The activities of the catalysts were determined during the hydrodenitrogenation of carbazole at 573 K and 10.1 MPa total pressure.  $\text{MoO}_2$ ,  $\gamma\text{-Mo}_2\text{N}$ , and Mo metal were mainly formed in the NH catalysts nitrated at 773, 973 and 1173 K, respectively. Mo oxides and metals in the NH catalysts were nitrated to  $\gamma\text{-Mo}_2\text{N}$  and  $\beta\text{-Mo}_2\text{N}_{0.78}$  with low crystallinity during TPD. The surface area of the NH and HE catalysts nitrated at 773 K increased to 66 and 59  $\text{m}^2 \text{g}^{-1}$  maximum from 1.1  $\text{m}^2 \text{g}^{-1}$  of fresh  $\text{MoO}_3$ , respectively, but decreased as the nitriding temperature increased to 973 K and 1173 K. The HE catalysts per surface area were more active than the NH catalysts for both the overall HDN reaction and hydrogenation, and the 1173 K-nitrated catalysts were highest. On the other hand, the NH catalysts were more active than the HE catalysts for C–N hydrogenolysis and the 973 K-nitrated catalyst showed a maximum activity for C–N hydrogenolysis. © 1998 Elsevier Science B.V. All rights reserved.

**Keywords:** Molybdenum Nitride; HDN; Carbazole; XRD; TPD

### 1. Introduction

The synthesis and structure of unsupported Mo nitride have been extensively studied. The catalytic properties of the Mo nitrides are governed by their bulk composition and surface structure. Since the large surface area of the material makes it a particu-

larly promising compound for heterogeneous catalysis, several methods for the preparation of refractory materials with large surface area have been developed; Volpe and Boudart [1] reported the synthesis of (fcc)  $\gamma\text{-Mo}_2\text{N}$  with a large surface area ( $180 \text{ m}^2 \text{g}^{-1}$ ) using the temperature-programmed reaction of  $\text{MoO}_3$  with  $\text{NH}_3$  in a range from 630 K to 980 K. Jagers et al. [2] also stressed the importance of the reaction intermediates in determining the surface areas and constituent phases. They found that the solid-state reaction of  $\text{MoO}_3$  with  $\text{NH}_3$  proceeds through two parallel reaction pathways:  $\text{MoO}_3 \rightarrow \text{MoO}_x\text{N}_{1-x} \rightarrow \gamma\text{-Mo}_2\text{N}$  and  $\text{MoO}_3 \rightarrow \text{MoO}_2 \rightarrow \gamma\text{-Mo}_2\text{N} + \delta\text{-MoN}$ . The formation of oxynitride,  $\text{MoO}_x\text{N}_{1-x}$ , resulted in a large increase

\*Corresponding author. Tel.: +81 423 887060; fax: +81 423 814201; e-mail: mnagai@cc.tuat.ac.jp

<sup>1</sup>Present address: R & D Department, Denka Chemical Co., 6 Goi-minami-Kaigan, Ichihara, Chiba 290, Japan.

<sup>2</sup>Present address: Bridgestone Co., 1 Kashiwao, Totsuka, Yokohama 244, Japan.

in surface area, which was due to the pseudomorphological nature of the reaction, while the formation of  $\text{MoO}_2$  and Mo metal led to smaller surface area materials. Much less attention has been given for examining the change in the surface structure and composition of the catalysts such as Mo and nitrogen species after treatment of the molybdena–alumina precursor in flowing  $\text{NH}_3$  or He gas.

Temperature-programmed desorption (TPD) is a useful technique for determining the presence of Mo and nitrogen species adsorbed on the catalyst surfaces. Gaseous products evolved from the catalysts characterize the Mo and nitrogen species of the catalysts during TPD. When TPD is used in combination with XRD measurements for unsupported or near-bulk Mo nitrides, they can provide further structural information on the Mo nitrides which coexist with the oxide, nitride and metal forms. In this work, the application of these techniques is demonstrated for the surface species and composition of the  $\text{MoO}_3$  treated with  $\text{NH}_3$  at 773, 973 and 1173 K, followed by cooling in  $\text{NH}_3$  or purging with He followed by cooling in He. The effects of the treatment after nitriding of the  $\text{MoO}_3$  on Mo and nitrogen species of the catalysts are determined. The activity and the selectivity of the catalysts are also studied for the HDN of carbazole at 573 K and 10.1 MPa total pressure.

## 2. Experimental

### 2.1. Catalyst preparation

Hydrogen and He (99.999%) were dried by passing them through Deoxo units (SUPELCO Oxyorb) and a Linde 13X molecular sieve trap prior to use.  $\text{NH}_3$  (99.999%) was used without further purification.  $\text{MoO}_3$  contained 97.1%  $\text{MoO}_3$  in 2.9%  $\gamma\text{-Al}_2\text{O}_3$  as a binder (Nikki Chemical). The mixed alumina and ammonium paramolybdate were molded into 3 mm o.d. pellets with a kneader. After being dried at 393 K for 24 h and then calcined at 823 K for 3 h, the pellets were crushed and sieved to 10–20 mesh (0.85–1.70 mm) granules for activity measurement, and ground for characterization of the catalysts. The  $\text{MoO}_3$  was packed on a fritted plate in a quartz microreactor, which consisted of a 20 mm long quartz

tubing of 10 mm o.d., attached at both sides with 50 mm long quartz tubing of 6 mm o.d. The  $\text{MoO}_3$  sample was heated at 723 K in air for 1 h and cooled to 573 K, and then nitrided with pure  $\text{NH}_3$  at  $49.6 \mu\text{mol s}^{-1}$  from 723 K to 773, 973 and 1173 K at a rate of  $1 \text{ K min}^{-1}$  and held at this temperature for 3 h. After nitriding two alternative treatments were performed. In the first, the sample was cooled from the nitriding temperature to room temperature in flowing  $\text{NH}_3$ . In the second treatment, the  $\text{NH}_3$  was switched to He gas at each of the three nitriding temperatures after nitriding. The sample was purged at 973 K in He for 1 h, and then cooled to room temperature in flowing He.

Abbreviated notations of the catalyst are used throughout this paper as shown in Table 1. For example, NH-L denoted 97.1%  $\text{Mo}/\text{Al}_2\text{O}_3$  nitrided at 773 K in  $\text{NH}_3$  for 3 h and followed by cooling to room temperature in flowing  $\text{NH}_3$ , while HE-H denotes 97.1 wt%  $\text{Mo}/\text{Al}_2\text{O}_3$  nitrided at 1173 K in  $\text{NH}_3$  for 3 h and followed by cooling to room temperature in flowing He after purged with He at 973 K for 1 h.

### 2.2. Analysis of surface area, nitrogen content, and molybdenum content

The specific surface area of the catalyst was measured by nitrogen adsorption using a standard volumetric BET apparatus after evacuation at 473 K and 1 Pa for 2 h. Nitrogen content was analyzed with a Perkin–Elmer CHN elemental analyzer for both the NH and He catalysts. Molybdenum analysis was done using atomic absorption spectroscopy.

### 2.3. Temperature-programmed desorption

TPD was performed for the nitrided catalysts under in situ conditions after preparation of the Mo nitrides. The nitrided catalyst was heated to room temperature in flowing He for 1 h after nitriding, and then heated to 1263 K at a rate of  $0.167 \text{ K s}^{-1}$  at a He flow of  $11.1 \text{ mmol s}^{-1}$ . The gases desorbed from the catalyst were monitored on-line using a quadrupole mass spectrometer (ULVAC, MSQ-150A) equipped with a variable-leak valve heated using heating tape about 350 K. The desorption rate of  $\text{N}_2$ ,  $\text{H}_2$ ,  $\text{NH}_3$  and water were calculated by calibration curves for each gas.

Table 1

The surface area and the amount of N<sub>2</sub> desorption from the samples during TPD

Sample <sup>a</sup>	Surface area <sup>b</sup> (m <sup>2</sup> g <sup>-1</sup> )	Desorption uptake of N <sub>2</sub> and H <sub>2</sub>					
		N <sub>2</sub> (mmol g <sup>-1</sup> )	NH <sub>3</sub> (mmol g <sup>-1</sup> )	Total N <sup>c</sup> (N <sub>2</sub> +NH <sub>3</sub> ) (mmol g <sup>-1</sup> )	H <sub>2</sub> (mmol g <sup>-1</sup> )	Total H (H <sub>2</sub> +H <sub>2</sub> O+NH <sub>3</sub> )	H/N
NH-L	66	0.88	0.03	0.90	0.19	0.57	0.26
HE-L	59	0.906	0.013	0.90	0.094	0.241	0.13
NH-M	33	0.54	0.05	0.565	0.09	0.40	0.71
HE-M	18	0.293	0.008	0.297	0.075	0.202	0.34
NH-H	8	1.63	0.09	1.68	0.105	0.77	0.23
HE-H	6	0.573	0.004	0.575	0.0113	0.0385	0.034

<sup>a</sup> The NH samples were cooled in flowing NH<sub>3</sub> to room temperature after nitriding a fresh MoO<sub>3</sub> sample (surface area, 1.1 m<sup>2</sup> g<sup>-1</sup>) to 773 K (L), 973 K (M), and 1173 K (H). The HE samples were nitrided at 773 K (L), 973 K (M), and 1173 K (H), purged in flowing He at 973 K for 1 h, and cooled in flowing He to room temperature.

<sup>b</sup> Evacuated at 473 K and at 1 Pa.

<sup>c</sup> N<sub>2</sub>: on a basis of N<sub>2</sub>.

## 2.4. X-ray diffraction

The changes in the composition of the catalysts were studied by interrupting the temperature program at the points corresponding to the labeled points (i.e., A, B, and C) in the TPD experiments. The compositions of the intermediate and final products were measured using XRD. X-ray diffraction powder analysis was performed with Ni-filtered CuK<sub>α</sub> radiation ( $\lambda=1.5418$  Å) using a Rigaku X-ray diffractometer operating at 30 kV and 20 mA with a scanning speed of 5° min<sup>-1</sup> from  $2\theta=5^\circ$  to  $2\theta=120^\circ$ .

## 2.5. Method of activity test

The HDN of carbazole was carried out in a high pressure flow system. The microreactor was a 325 mm long stainless steel tube of 17.3 mm o.d. and 3.2 mm thickness. The HDN of carbazole on the nitrided HE and NH catalysts was conducted at 573 K and 10.1 MPa in a down-flow fixed-bed microreactor using 0.25 wt.% carbazole in xylene. Catalyst loadings were 2.0 g. Products of the reaction were quantitatively analyzed using FID gas chromatography with 1% Silicone OV-17 [3]. The rates of conversion of carbazole (overall HDN rate), the formation of the denitrogenated compounds (C–N hydrogenolysis rate), and of the hydrogenated carbazole compounds (hydrogenation rate), were calculated and reported as molecules h<sup>-1</sup> m<sup>-2</sup>.

## 3. Results and discussion

### 3.1. BET surface area

The surface areas of the NH and HE catalysts are shown in Table 1. The surface area of the NH catalyst increased to 66 m<sup>2</sup> g<sup>-1</sup> from 1.1 m<sup>2</sup> g<sup>-1</sup> after a nitriding treatment of 773 K for the fresh sample, but decreased to 33 m<sup>2</sup> g<sup>-1</sup> as nitriding temperature increased from 773 K to 1173 K. For the HE catalysts, the surface areas showed the same trend of decreasing surface area with increasing nitriding temperature of the NH<sub>3</sub>-cooled catalysts. The NH catalysts had a higher surface area than the HE catalysts at the same nitriding temperature. It appears that cooling of the nitrided catalysts in NH<sub>3</sub> makes smaller particles and better heterogeneity of the surface than that in He. For both the NH<sub>3</sub> and He treated catalysts, a higher nitriding treatment lowered the surface area of the catalysts, because of sintering of the catalysts at high temperature.

### 3.2. Changes in the composition of 773 K-nitrided catalyst during TPD

The TPD profile for the NH-L catalyst is shown in Fig. 1(a). The TPD shows one large peak of N<sub>2</sub> desorption at 778 K with peaks at 978 and 1034 K. The peak of N<sub>2</sub> desorption at the low temperature was accompanied by one peak of H<sub>2</sub> desorption at the

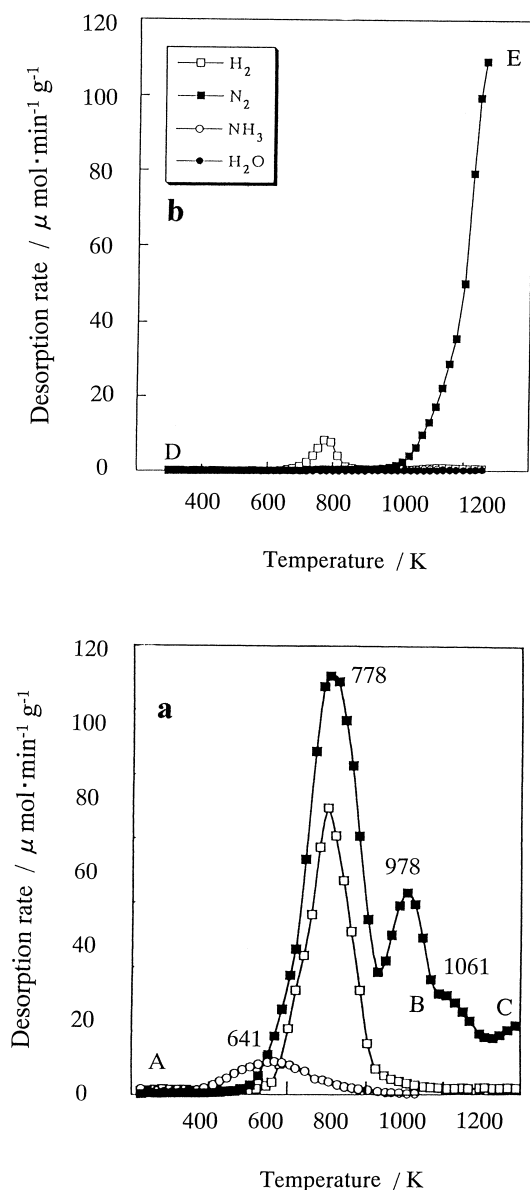


Fig. 1. Temperature-programmed desorption of the (a) NH-L and (b) HE-L catalyst. (■)  $\text{N}_2$ , (□)  $\text{H}_2$ , (○)  $\text{NH}_3$ , and (●)  $\text{H}_2\text{O}$ .

magnitude of 60%  $\text{N}_2$  desorption. When adsorbed  $\text{NH}_3$  was decomposed to release  $\text{N}_2$  and  $\text{H}_2$  from the catalyst during TPD, the molar ratio of  $\text{H}_2$  to  $\text{N}_2$  gave a stoichiometric value of 3.0. If  $\text{MoO}_3$  was reduced to  $\text{MoO}_2$  with  $\text{H}_2$  desorbed from the catalyst, water was evolved. However, no water was formed in the TPD. From this result, the adsorbed nitrogen

species contain nonstoichiometric  $\text{NH}_x$  ( $x < 3$ ), which reacts and rearranges on the surface to desorb  $\text{N}_2$  and  $\text{H}_2$ . In this TPD experiment, the desorption of  $\text{H}_2\text{O}$  was significant with NH-L but scarcely observed for the other catalysts. The XRD analysis for the NH-L and HE-L showed the presence of  $\text{MoO}_2$  in Fig. 2.  $\text{H}_2\text{O}$  ought to have been formed during TPD if Mo oxynitride was decomposed below 1000 K. The only other possibility is the formation of Mo oxynitride in the NH-L which desorbed  $\text{H}_2\text{O}$  above 1123 K during TPD.

The X-ray powder diffraction analysis was undertaken to determine the composition and crystallinity of the intermediates during TPD. For the NH-L catalyst, the as-prepared catalyst did not consist of  $\gamma\text{-Mo}_2\text{N}$  but  $\text{MoO}_2$  with low intensity (1 K cps), as shown in Fig. 2(A). When the catalyst was heated to 933 K (Point B),  $\text{MoO}_2$  was slightly altered to  $\gamma\text{-Mo}_2\text{N}$  (Fig. 2(B)) with low crystallinity (0.5 K cps) while desorbing  $\text{N}_2$  gas. Further heating to 1270 K (Point C) enhanced the growth of  $\beta\text{-Mo}_2\text{N}_{0.78}$  and  $\gamma\text{-Mo}_2\text{N}$ , although  $\text{MoO}_2$  was still present as a major compound with large crystallinity (5 K cps). These results suggested that the second peak of  $\text{N}_2$  desorption at 1034 K was due to the release of  $\text{N}_2$  gas during the transformation of  $\gamma\text{-Mo}_2\text{N}$  to  $\beta\text{-Mo}_2\text{N}_{0.78}$ .  $\text{NH}_x$  adsorbed on the NH-L catalyst was expected to affect the composition and structure of the sample during TPD. From the XRD analysis,  $\text{NH}_x$  adsorbed on the catalyst nitrified  $\text{MoO}_2$  to form  $\gamma$ - and  $\beta\text{-Mo}_2\text{N}_{0.78}$  during TPD and lowered to XRD intensity of  $\text{MoO}_2$  by forming small particles of  $\text{MoO}_2$ . NH catalysts have larger surface areas than HE catalysts, consistent with the hypothesis of small particles. We believe that Mo oxide, nitride, and metal particles on the NH catalyst became smaller when nitrogen species such as  $\text{NH}_x$  ( $x=0\sim3$ ) accumulated and adsorbed on the catalyst during cooling in flowing  $\text{NH}_3$ .

For the HE-L catalyst, the TPD profile (Fig. 1(b)) and XRD pattern (Fig. 2(D) and (E)) are significantly different from those for the NH-L catalyst. No large  $\text{N}_2$  peak was observed at 818 K but the desorption of  $\text{N}_2$  was significantly increased above 1000 K during TPD. The intensity of the XRD pattern for the HE-L catalyst was extremely high (8 K cps in Point D in Fig. 1(b)). The process, an annealing of the catalysts purged and cooled to room temperature in flowing He, resulted in good crystallinity of  $\text{MoO}_2$ . The catalyst,

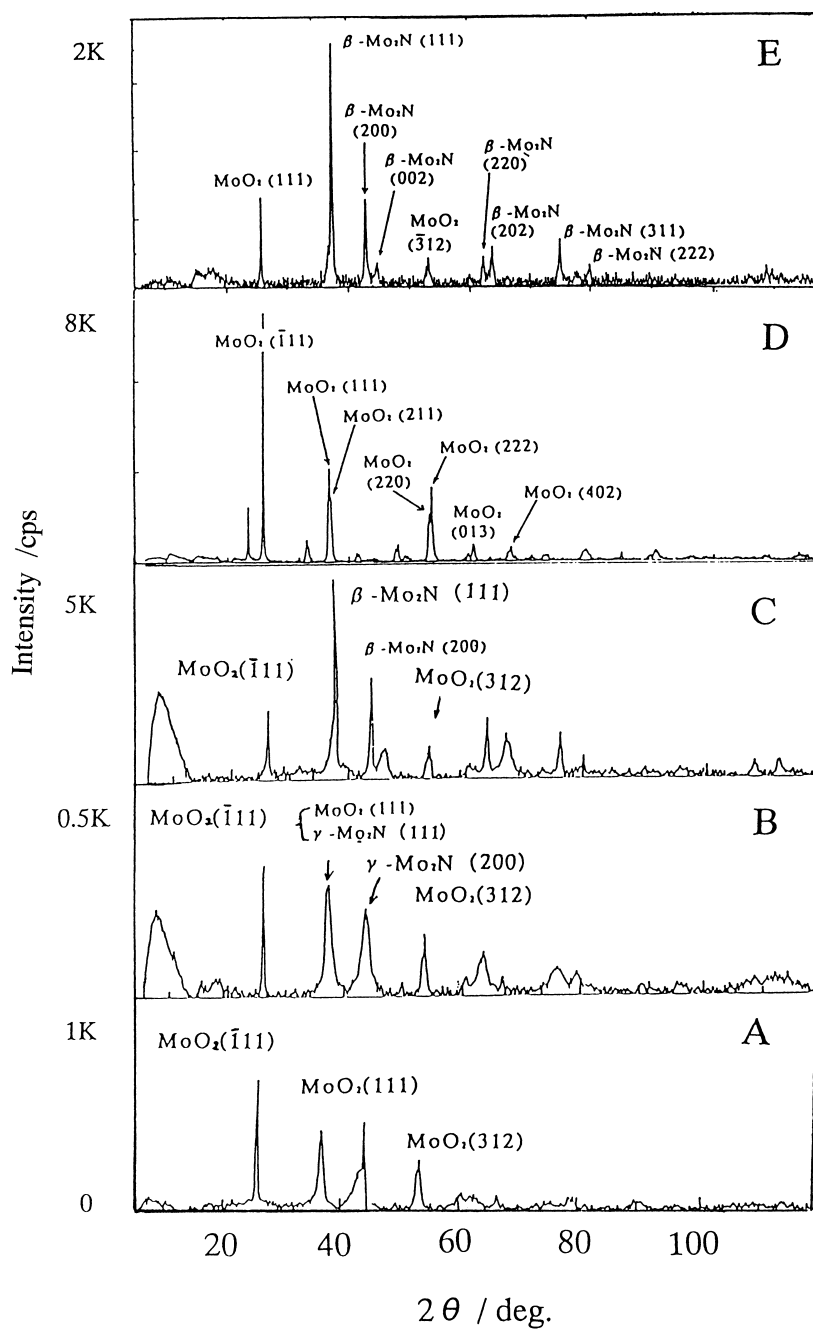


Fig. 2. XRD patterns of NH-L and HE-L catalysts. (A) As-prepared NH-L sample (point A in Fig. 1(a)), (B) the intermediate heated to 1013 K (point B in Fig. 1(a)), (C) the sample at 1270 K (point C in Fig. 1(a)), (D) as-prepared HE-L sample (Point D in Fig. 1(b)), (E) the sample at 1202 K (point E in Fig. 1(b)).

heated to 1270 K (point E in Fig. 1(b)), contained  $\beta$ - $\text{Mo}_2\text{N}_{0.78}$  and  $\text{MoO}_2$  but not  $\gamma$ - $\text{Mo}_2\text{N}$  as shown in Fig. 2(E). There is probably a route for the direct nitridation of  $\text{MoO}_2$  to  $\beta$ - $\text{Mo}_2\text{N}_{0.78}$  with adsorbed  $\text{NH}_x$ , but no direct route from  $\gamma$ - $\text{Mo}_2\text{N}$  to  $\beta$ - $\text{Mo}_2\text{N}_{0.78}$  for the HE-L catalyst during TPD. In contrast, for the NH-L catalyst,  $\text{MoO}_2$  was nitrided to form  $\beta$ - $\text{Mo}_2\text{N}_{0.78}$  from  $\gamma$ - $\text{Mo}_2\text{N}$  formed during the topotactic rearrangement of  $\text{MoO}_2$  [2] with adsorbed  $\text{NH}_x$  and  $\text{NH}_3$ . Moreover, a small desorption peak of  $\text{H}_2$  at 780 K without  $\text{N}_2$  was observed for the HE-L catalyst, suggesting the consumption of all the nitrogen content of adsorbed  $\text{NH}_x$  for the nitriding of  $\text{MoO}_2$  to  $\beta$ - $\text{Mo}_2\text{N}_{0.78}$ . The amount of desorbed  $\text{N}_2$  from room temperature to 1270 K was  $0.88 \text{ mmol g}^{-1}$  on the basis of  $\text{N}_2$  as shown in Table 1. This value is consistent with nitriding 4.9% Mo atoms of the  $\text{Mo}/\text{Al}_2\text{O}_3$  when  $\text{MoO}_3$  was completely converted to  $\beta$ - $\text{Mo}_2\text{N}_{0.78}$ .

### 3.3. Changes in the composition of 973 K-nitrided catalyst during TPD

The TPD profile for the NH-M catalyst at 973 K is shown in Fig. 3(a). The NH-M catalyst had a smaller peak of  $\text{N}_2$  desorption than the NH-L catalyst. Two peaks of  $\text{N}_2$  desorption were observed at 819 K and 1001 K.  $\text{N}_2$  for the low-temperature peak was accompanied by  $\text{H}_2$ .  $\text{NH}_3$  and  $\text{H}_2\text{O}$  were barely detectable. The peaks of  $\text{N}_2$  and  $\text{H}_2$  gases at 819 K were due to the decomposition and rearrangement of  $\text{NH}_x$  adsorbed in the NH-M catalyst.  $\text{N}_2$  desorption at 1001 K was accompanied by changes in the XRD patterns. The XRD patterns of intermediates during TPD for the NH-M catalyst are depicted in Fig. 4. When the as-prepared sample,  $\gamma$ - $\text{Mo}_2\text{N}$  (Fig. 4(F)), was heated to 1073 K (G) and 1159 K (H),  $\gamma$ - $\text{Mo}_2\text{N}$  was transformed to  $\beta$ - $\text{Mo}_2\text{N}_{0.78}$  with a high crystallinity (Fig. 4(H)). Therefore, the XRD analysis for the HE-M catalyst showed that the  $\text{N}_2$  desorption without  $\text{H}_2$  at the broad peak of 1001 K was due to the release of  $\text{N}_2$  during the transformation of  $\gamma$ - $\text{Mo}_2\text{N}$  to  $\beta$ - $\text{Mo}_2\text{N}_{0.78}$ .

On the other hand, the HE-M catalyst showed only one small peak of  $\text{N}_2$  desorption at 1040 K and a gradual increase in  $\text{N}_2$  desorption with a desorption temperature above 1040 K as shown in Fig. 3(b). The change in the composition of the HE-M catalyst at 1040 K was estimated as follows. The as-prepared HE-M catalyst was comprised of  $\beta$ - $\text{Mo}_2\text{N}_{0.78}$

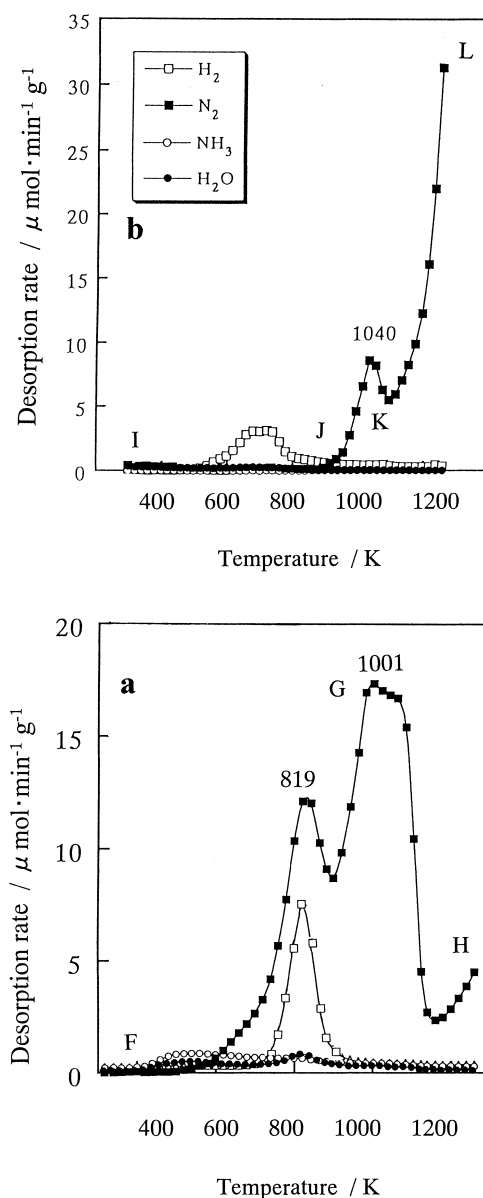


Fig. 3. TPD of the (a) NH-M and (b) HE-M catalysts. (■)  $\text{N}_2$ , (□)  $\text{H}_2$ , (○)  $\text{NH}_3$ , and (●)  $\text{H}_2\text{O}$ .

(Fig. 4(I)), indicating that  $\gamma$ - $\text{Mo}_2\text{N}$  turned to  $\beta$ - $\text{Mo}_2\text{N}_{0.78}$  by purging in flowing He at 973 K for 1 h and subsequently cooling to room temperature. In contrast, when the sample was cooled in flowing  $\text{NH}_3$  after nitriding at 973 K,  $\gamma$ - $\text{Mo}_2\text{N}$  remained unchanged. Although  $\beta$ - $\text{Mo}_2\text{N}_{0.78}$  (Fig. 4(I)) was converted to  $\gamma$ - $\text{Mo}_2\text{N}$  at 950 K (Fig. 4(J)) during TPD, the

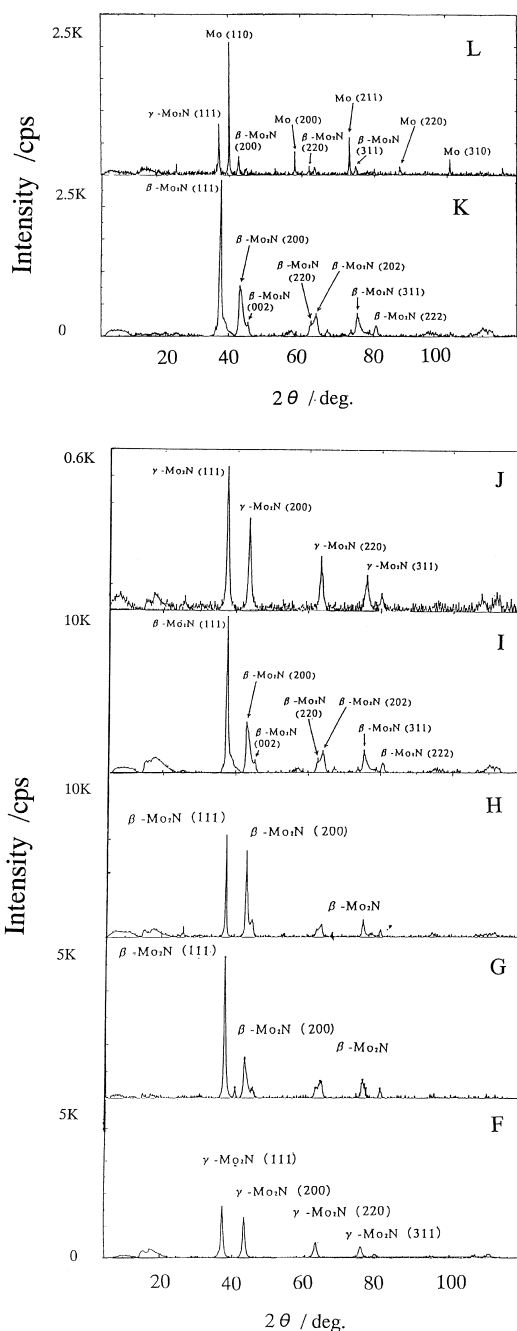
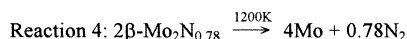
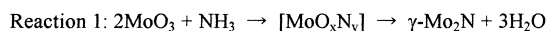
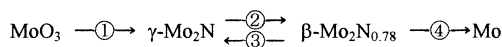


Fig. 4. XRD patterns of NH-M and HE-M catalysts. (F) As-prepared NH-M sample (point F in Fig. 3(a)), (G) the intermediate heated to 1073 K (point G in Fig. 3(a)), (H) the intermediate heated to 1159 K (point H in Fig. 3(a)), (I) as-prepared HE-M sample (Point I in Fig. 3(b)), (J) the intermediate heated to 975 K (point J in Fig. 3(b)) (K) heated to 1073 K (point K in Fig. 3(b)), (L) heated 1159 K (point L in Fig. 3(b)).



Scheme 1.

catalyst was again changed to  $\beta\text{-Mo}_2\text{N}_{0.78}$  at 1100 K (Fig. 4(K)). This transformation of the catalyst between 900 K and 1100 K ( $\gamma\text{-Mo}_2\text{N}$  to  $\beta\text{-Mo}_2\text{N}_{0.78}$ ) was also observed for the NH-L catalysts. Therefore, the peak in the range of 900 K and 1100 K is due to the desorption of  $\text{N}_2$  during the transformation of  $\gamma\text{-Mo}_2\text{N}$  to  $\beta\text{-Mo}_2\text{N}_{0.78}$  (Fig. 4(K)). Upon further heating to 1206 K, a part of  $\beta\text{-Mo}_2\text{N}_{0.78}$  was altered to Mo metal (Fig. 4(L)). This result suggested that the  $\text{N}_2$  desorption above 1100 K for the HE-M catalyst was ascribed to the liberation of  $\text{N}_2$  gas during the reduction of  $\beta\text{-Mo}_2\text{N}_{0.78}$  to Mo metal. Thus, adsorbed nitrogen and  $\text{NH}_x$  species make Mo nitrides and oxides unstable to form smaller particles during the heating process (Scheme 1).

### 3.4. Changes in the composition of 1173 K-nitrided catalyst during TPD

The TPD profile for the NH-H catalyst is shown in Fig. 5(a). One strong peak of  $\text{N}_2$  desorption was observed at 1135 K with a shoulder peak at 1025 K. In the XRD data of the catalysts at that temperature, (Point M in Fig. 5(a)), the as-prepared catalyst (Fig. 6(M)) contained Mo metal (mainly Mo (110)) with a small amount of  $\beta\text{-Mo}_2\text{N}_{0.78}$ . However, when the as-prepared catalyst was heated to 773 K (Point N in Fig. 5(a)) a part of the Mo metal was altered to  $\beta\text{-Mo}_2\text{N}_{0.78}$  that grew with very low crystallinity (Fig. 6(N)). Upon further heating to 1273 K (Point O),  $\beta\text{-Mo}_2\text{N}_{0.78}$  completely changed to Mo metal again with the recovery of about 70% of its crystallinity after the desorption of  $\text{N}_2$  during TPD. This result supported the reduction of  $\beta\text{-Mo}_2\text{N}_{0.78}$  to Mo metal at ca. 1135 K. Adsorbed  $\text{NH}_x$  appears to make  $\text{Mo}_2\text{N}$  susceptible to reduction. The peak of  $\text{N}_2$  desorption at 1025 K for NH-H corresponded with that at

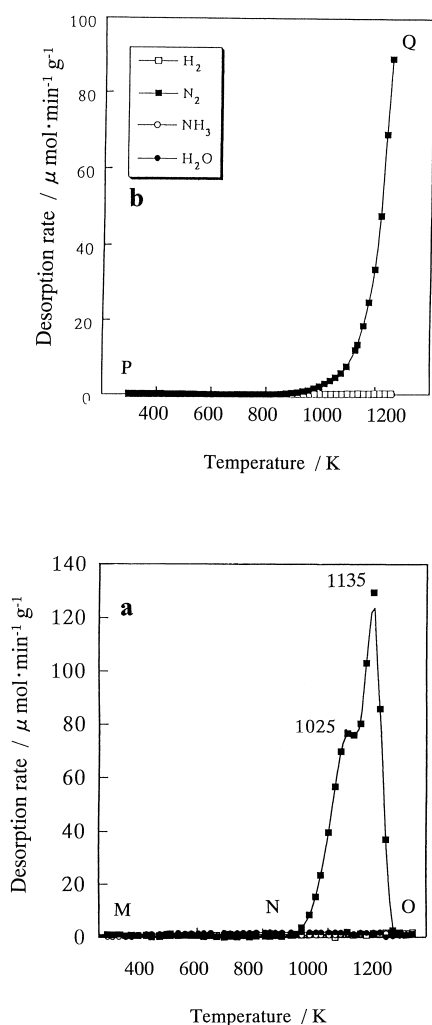


Fig. 5. TPD of the (a) NH-H and (b) HE-H catalysts. (■)  $\text{N}_2$ , (□)  $\text{H}_2$ , (○)  $\text{NH}_3$ , and (●)  $\text{H}_2\text{O}$ .

1034 K for the NH-L and those at 1001 K for the NH-M and HE-M catalysts. Therefore, the major peak of  $\text{N}_2$  desorption at 1135 K and the shoulder peak at 1025 K were due to the release of  $\text{N}_2$  during the reduction of  $\beta\text{-Mo}_2\text{N}_{0.78}$  to Mo metal and the transformation of  $\gamma\text{-Mo}_2\text{N}$  to  $\beta\text{-Mo}_2\text{N}_{0.78}$ , respectively. The amount of  $\text{N}_2$  desorbed on heating NH-H to 1159 K during TPD corresponded to 9% of  $\text{MoO}_3$  in the Mo/ $\text{Al}_2\text{O}_3$  being converted to  $\beta\text{-Mo}_2\text{N}_{0.78}$ . Furthermore, neither  $\text{H}_2$  nor  $\text{H}_2\text{O}$  were desorbed from the catalyst between 300 K and 1270 K. This result indicates that nitrogen but not  $\text{NH}_x$  ( $x=1\sim3$ ) or hydrogen were

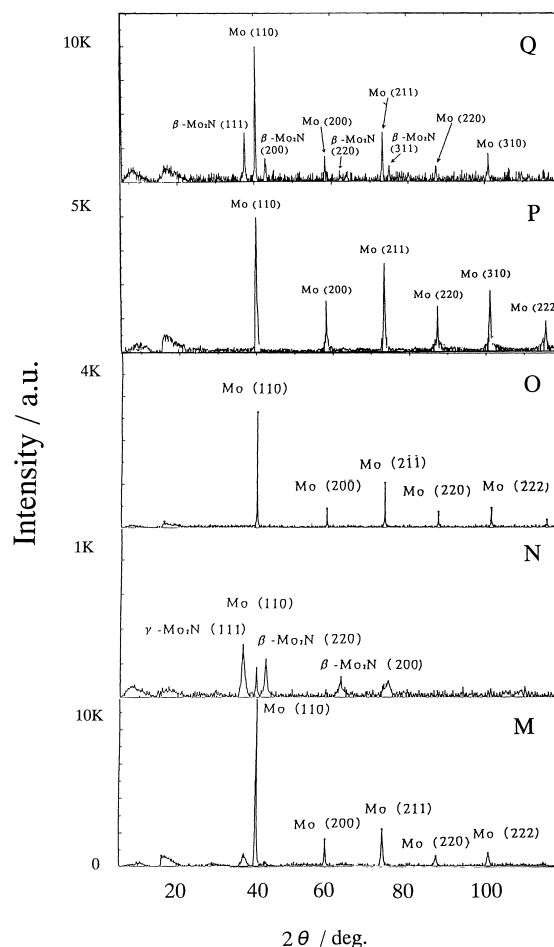


Fig. 6. XRD patterns of the NH-H and HE-H catalysts. (M) As-prepared NH-H (point M in Fig. 5(a)), (N) intermediate at 773 K (point N in Fig. 5(a)), (O) at 1200 K (point O in Fig. 5(a)), (P) as-prepared HE-H sample (Point P in Fig. 5(b)), (Q) at 1257 K (point Q in Fig. 5(b)).

present in NH-H. Han and Schmidt [4] reported that no  $\text{H}_2$  above 600 K in flash desorption spectra on Mo (100). Bafrali and Bell [5] also found no  $\text{H}_2$  desorbed from Mo metal (100) above 600 K during TPD, though  $\text{H}_2$  was evolved at 177, 227 and 300 K.

On the other hand, for the HE-H catalyst (Point P in Fig. 5(b)), the desorption of  $\text{N}_2$  was not observed below 850 K but sharply increased above 850 K. The as-prepared catalyst (P in Fig. 5(b)) was composed of Mo metal with low crystallinity (Fig. 6(P)). When the as-prepared catalyst reached 1257 K, XRD revealed highly crystalline Mo metal together with a



small amount of  $\beta\text{-Mo}_2\text{N}_{0.78}$  (Fig. 6(Q)). Table 1 shows that  $\text{H}_2$  was produced from the HE-L and HE-M catalysts but not from the HE-H catalyst, indicating that  $\text{NH}_x$  was present on the Mo oxides and nitrides. However,  $\text{NH}_x$  was not adsorbed on Mo metal but nitrogen was. Adsorbed nitrogen species nitride Mo oxides and Mo metals to form small particles. Oyama and Boudart [6] also reported that molybdenum powder takes up nitrogen after ammonia synthesis corresponding to 4 or 5 layers of  $\text{Mo}_2\text{N}$ . Adsorbed atomic nitrogen is reported to be desorbed from polycrystalline molybdenum [7,8] at about 1210 K [9]. The strength of N adsorption is confirmed by the fact that  $\text{N}_2$  desorbs from nitrified Mo(100) at only above 1200 K. Maning and Schmidt also reported that  $\text{N}_2$  on Mo(110) desorbs from a single binding state at a peak temperature of 1460 K [10]. Matsushita and Hansen [7] reported that nitrogen is adsorbed by clean Mo metal (110) in two well-defined states: one stable up to 1273 K, and the other one stable only below 130 K. Furthermore, on Mo(100), there are two peaks, one at 1350 K [5], the other at 193 K. In conclusion, the He-cooled catalysts are annealed highly crystalline products from which  $\text{NH}_x$  has been purged during the change from  $\gamma\text{-Mo}_2\text{N}$  to  $\beta\text{-Mo}_2\text{N}_{0.78}$ , whereas the NH catalysts remain polycrystalline in the presence of  $\text{NH}_3$  gas and adsorbed  $\text{NH}_x$ . The XRD data on NH catalysts indicates Mo oxides remained on the as-prepared NH-L catalyst but Mo nitrides were formed in the NH-M catalyst. Desorption at 820–845 K of  $\text{N}_2$  and  $\text{H}_2$  are due to adsorbed  $\text{NH}_x$ . In the NH-L catalysts, the second peak in the TPD arises from the evolution of  $\text{N}_2$  during the transformation of  $\gamma\text{-Mo}_2\text{N}$  to  $\beta\text{-Mo}_2\text{N}_{0.78}$ .

### 3.5. Catalyst test

The major denitrogenated product was bicyclohexyl together with small amount of cyclohexylhexene and hexylcyclohexane. The primary hydrogenated product was tetrahydrocarbazole, but traces of other hydrogenated carbazole compounds such as hexahydrocarbazole, octahydrocarbazole, and perhydrocarbazole were observed. The rates for the C–N hydrogenolysis and hydrogenation in the HDN of carbazole are given in Figs. 7 and 8, respectively. The results are also given in Table 2. The rate of the hydrogenation for the HE catalysts increased with

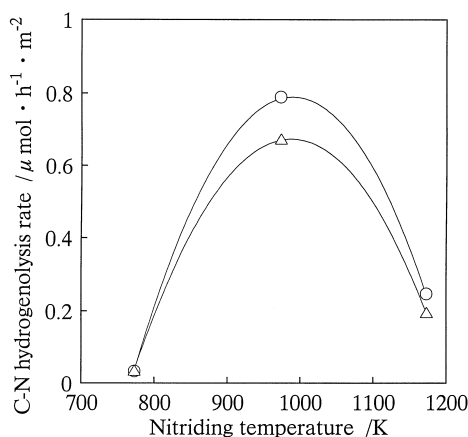


Fig. 7. The C–N hydrogenolysis rates of the (○) NH and (△) HE catalysts for the HDN of carbazole at 573 K and 10.1 MPa total pressure.

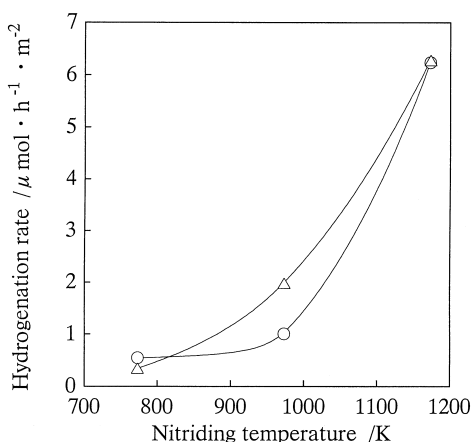


Fig. 8. The hydrogenation rates of the (○) NH and (△) HE catalysts for the HDN of carbazole at 573 K and 10.1 MPa total pressure.

increasing nitriding temperature and exhibited a greater rate than those for the NH catalysts. The HE-H was the most active in the hydrogenation of carbazole. For the C–N hydrogenolysis, the activity of the NH catalyst was greater than that of the HE, and the NH-M was the most active.

### 3.6. Mo species and HDN activity

The NH-M catalyst was the most active for C–N hydrogenolysis of carbazole and the HE-M catalyst exhibited the second highest activity. The NH-M

Table 2  
HDN of carbazole at 573 K and 10.1 MPa

Catalyst nitriding temperature	Overall <sup>a</sup>			C–N hydrogenolysis <sup>b</sup>			Hydrogenation <sup>c</sup>		
	(μ mol h <sup>-1</sup> m <sup>-2</sup> )		NH/He	(μ mol h <sup>-1</sup> m <sup>-2</sup> )		NH/He	(μ mol h <sup>-1</sup> m <sup>-2</sup> )		NH/He
	NH <sup>d</sup>	HE <sup>e</sup>		NH	HE		NH	HE	
773 K	0.389	0.489	0.796	0.0326	0.0356	0.916	0.547	0.348	0.152
973 K	1.76	2.63	0.669	0.789	0.674	1.17	1.00	1.98	0.505
1173 K	3.94	4.36	0.904	0.248	0.197	1.26	6.24	6.28	0.993

<sup>a</sup> Overall HDN rate; based on the conversion of carbazole.

<sup>b</sup> Based on the formation of the denitrogenated compounds.

<sup>c</sup> Based on the conversion of carbazole.

<sup>d</sup> The sample was cooled in flowing NH<sub>3</sub> to room temperature after nitriding.

<sup>e</sup> The sample was cooled in flowing He to room temperature, after the sample was purged with He at 973 K for 1 h.

catalyst consisted of  $\gamma$ -Mo<sub>2</sub>N but the HE-M contained  $\gamma$ -Mo<sub>2</sub>N<sub>0.78</sub>. Purging the samples with He converted  $\gamma$ -Mo<sub>2</sub>N to  $\beta$ -Mo<sub>2</sub>N<sub>0.78</sub> in HE-M. The compositions of NH-M and HE-M did not change significantly at 573 K. XRD analysis indicated the transformation of  $\beta$ -Mo<sub>2</sub>N<sub>0.78</sub> in NH-M at 1001 K (Fig. 3(a)) and that of  $\gamma$ -Mo<sub>2</sub>N in HE-M at 800 K (Fig. 3b). Moreover, the HE-H catalyst was the most active for the hydrogenation. Lower amount of reduced Mo are created on the 973 K-nitrided catalyst than on the 1173 K-nitrided catalyst. Since the HE-H was comprised of Mo metal with a small amount of  $\beta$ -Mo<sub>2</sub>N<sub>0.78</sub>, the HE-H catalyst had patches of Mo metal species formed by NH<sub>3</sub> treatment at 1173 K. From the results,  $\gamma$ -Mo<sub>2</sub>N was most active in the C–N hydrogenolysis,  $\beta$ -Mo<sub>2</sub>N<sub>0.78</sub> less so, and MoO<sub>2</sub> least. Mo metal in HE-H was highly active for hydrogenation. MoO<sub>2</sub> in the NH-L was not as active as Mo metals and Mo nitrides for the C–N hydrogenolysis and hydrogenation during the HDN of carbazole. Furthermore, the amorphous MoO<sub>2</sub> in NH-L may make it more active than the HE-L for the hydrogenation of carbazole as shown in Fig. 8.

### 3.7. Nitrogen amount and nitrogen species

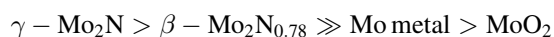
The NH catalyst, which was cooled to room temperature in flowing NH<sub>3</sub> after nitriding, held much more nitrogen, as shown in Table 1. The total amount of N<sub>2</sub> desorbed on heating the NH-L catalyst to 1159 K was 0.90 mmol g<sup>-1</sup>. Hillis et al. [11] reported that molybdenum dioxide adsorbed 1.89 mmol N<sub>2</sub>/g-MoO<sub>2</sub> for 10 h at 773 K. NH-L, comprised mainly of MoO<sub>2</sub>, desorbed half of this amount. The NH-H

catalyst, consisting of Mo metal desorbed 1.68 mmol N<sub>2</sub>/g-MoO<sub>2</sub> while NH-M consisting of  $\gamma$ -Mo<sub>2</sub>N desorbed 0.565 mmol N<sub>2</sub>/g-MoO<sub>2</sub>. Aika and Ozaki [12] reported that 1.92 mmol g/Mo of N<sub>2</sub> was adsorbed on a reduced molybdenum metal after 69 h of nitriding in N<sub>2</sub> at 775 K. Bell et al. [13,14] also reported that the uptake of NH<sub>3</sub> on  $\gamma$ -Mo<sub>2</sub>N with a large surface area (140–155 m<sup>2</sup> g<sup>-1</sup>) at 295 K is 0.77 mmol g<sup>-1</sup>. Our result of the amount of adsorbed nitrogen was less than those in the literature by a factor of 0.7–0.9 because of the 3 h nitriding time.

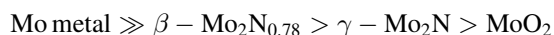
The N<sub>2</sub> desorption was thought to proceed through the recombination of adsorbed nitrogen on the surface [9]. Above 573 K, adsorbed NH<sub>3</sub> underwent sequential dehydrogenation to produce NH<sub>2</sub> and NH groups as well as N and H atoms [15,16]. The adsorption of strongly-bound H atoms, in small islands, could limit the availability of hydrogen in surface reactions [15]. Hydrogen was formed during the decomposition of NH<sub>3</sub> during cooling in flowing NH<sub>3</sub>. The NH catalysts contained more NH<sub>x</sub> ( $x < 1.5$ ) on the surface of the NH catalyst, but the HE catalysts contained less hydrogen in NH<sub>x</sub> as shown in Figs. 1, 3 and 5. In the present study, nitrogen is present as an adsorbed NH<sub>2</sub> group and N atoms on the surface of  $\gamma$ -Mo<sub>2</sub>N and alumina for the Mo/Al<sub>2</sub>O<sub>3</sub> catalyst nitrided at 973 K. Furthermore, NH<sub>3</sub> was decomposed on both Mo(100) and nitrided Mo(100) [5], while the two steps NH<sub>3</sub> (s)→NH<sub>2</sub> (s)→NH (s) are reversible, the third (NH (s)→N (s) + H (s)) is irreversible, reflecting the strong bonding of N<sub>s</sub>. Thus, N<sub>2</sub> was desorbed from the decomposition and reconstruction of NH<sub>x</sub> on the nitrided catalysts below 1150 K.

#### 4. Conclusions

1. TPD experiments indicated that  $\text{NH}_x$  species are present on the surface of the nitrated catalysts and react with  $\text{MoO}_2$  and Mo metal to form  $\gamma\text{-Mo}_2\text{N}$  and  $\beta\text{-Mo}_2\text{N}_{0.78}$ , respectively, during the TPD run.
2. The XRD measurement showed that molybdenum nitride is formed as  $\gamma\text{-Mo}_2\text{N}$  in the NH-M catalyst. For the catalysts nitrated at 773 K, there was no formation of molybdenum nitride on the surface.
3. The NH-L, -M and -H catalysts show three peaks for  $\text{N}_2$  desorption. A large first peak of  $\text{N}_2$  desorption at about 820 K was ascribed to the formation of  $\text{N}_2$  accompanied with  $\text{H}_2$ , during the combination and reaction of adsorbed NH and N species on the Mo surface. The second shoulder peak of  $\text{N}_2$  desorption at 1025–1054 K was due to the desorption of  $\text{N}_2$  from adsorbed nitrogen on  $\gamma\text{-Mo}_2\text{N}$  or  $\text{MoO}_2$  in the  $\text{NH}_3$ -cooled sample. The third  $\text{N}_2$  peak at 1135 K was due to the evolution of  $\text{N}_2$  during the transformation of  $\gamma\text{-Mo}_2\text{N}$  to  $\beta\text{-Mo}_2\text{N}_{0.78}$ .
4. Mo species was active in the C–N hydrogenolysis as follows:



5. Mo species was active in the hydrogenation as follows:



#### Acknowledgements

We are grateful for the Grant-In-Aid for Scientific Research of the Ministry of Education, Grant No. 07044132.

#### References

- [1] L. Volpe, M. Boudart, J. Phys. Chem. 90 (1986) 4874.
- [2] C.H. Jagers, J.N. Michaels, A.M. Stacy, Chem. Mater. 2 (1990) 150.
- [3] M. Nagai, T. Masunaga, N. Hanaoka, J. Catal. 101 (1986) 284.
- [4] H.R. Han, L.D. Schmidt, J. Phys. Chem. 75 (1971) 227.
- [5] R. Bafrali, A.T. Bell, Surf. Sci. 278 (1992) 353.
- [6] S.T. Oyama, M. Boudart, J. Res. Inst. Catal., Hokkaido Univ. 28 (1980) 305.
- [7] K. Matsushita, R.S. Hansen, J. Chem. Phys. 54 (1971) 2278.
- [8] D.D. Eley, S.H. Russell, Proc. Roy. Soc. London A341 (1974) 31.
- [9] M. Boudart, C. Egawa, S.T. Oyama, K. Tamaru, J. Chim. Phys. 78 (1981) 987.
- [10] M. Mahnig, L.D. Schmidt, Zeit. Phys. Chem. Neue Folge 80 (1972) 71.
- [11] M.R. Hillis, C. Kemball, M.W. Roberts, Trans. Faraday Soc. 63 (1967) 3570.
- [12] K. Aika, A. Ozaki, J. Catal. 14 (1969) 311.
- [13] G.W. Haddix, D.H. Jones, J.A. Reimer, A.T. Bell, J. Catal. 112 (1988) 556.
- [14] P.A. Armstrong, A.T. Bell, J.A. Reimer, J. Phys. Chem. 97 (1993) 1952.
- [15] G.W. Haddix, J.A. Reimer, A.T. Bell, J. Catal. 108 (1987) 50.
- [16] G.W. Haddix, A.T. Bell, J.A. Reimer, J. Phys. Chem. 93 (1989) 5859.